Analyst

Check for updates

Self-assembled two-dimensional gold nanoparticle film for sensitive nontargeted analysis of food additives with surface-enhanced Raman spectroscopy†

Yiping Wu, [ID] *[a] Wenfang Yu,[a] Benhong Yang[a] and Pan Li*[b]

The use of different food additives and their active metabolites has been found to cause serious problems to human health. Thus, considering the potential effects on human health, developing a sensitive and credible analytical method for different foods is important. Herein, the application of solvent-driven self-assembled Au nanoparticles (Au NPs) for the rapid and sensitive detection of food additives in different commercial products is reported. The assembled substrates are highly sensitive and exhibit excellent uniformity and reproducibility because of uniformly distributed and high-density hot spots. The sensitive analyses of ciprofloxacin (CF), diethylhexyl phthalate (DEHP), tartrazine and azodicarbonamide at the 0.1 ppm level using this surface-enhanced Raman spectroscopy (SERS) substrate are given, and the results show that Au NP arrays can serve as efficient SERS substrates for the detection of food additives. More importantly, SERS spectra of several commercial liquors and sweet drinks are obtained to evaluate the addition of illegal additives. This SERS active platform can be used as an effective strategy in the detection of prohibited additives in food.

Introduction

Food safety issues have attracted increasing attention in recent years.[1,2] Typically, illegal addition involves excessive addition of pigments, overuse of antibiotic drugs and pesticides in food products, *etc*.[3] All these illegal additions pose great threats to human health. For example, it is reported that phthalic acid esters may alter the methylation status of DNA and the DNA sequence itself, thus transmitting these effects to future generations.[4] Another example is that the abuse of Ciprofloxacin antibiotic may cause severe liver damage and hematuria.[5] Thus, several analytical strategies have been developed to obtain sensitive detection of food additives. Yuan *et al.* have reported an enzyme-linked immunosorbent assay (ELISA) to detect ciprofloxacin (CF) in food animal edible tissues at the nM level.[6] Gopal Das *et al.* investigated a pigment system through sharp colorimetric as well as fluorogenic responses in both physiological conditions and food additives.[7] However, the widely adopted analytical strategy is 'separation and detection',

which includes liquid chromatography (LC), capillary electrophoresis (CE), capillary electro-chromatography coupled with UV detection and electrochemical detection. On one hand, these methods require long operation times and exhibit limited spatial resolutions. On the other hand, these methods only focus on targeted compounds. To avoid health risks from illegal additives, it is necessary to develop nontargeted analysis methods for the rapid and sensitive detection of food additives.

Surface-enhanced Raman spectroscopy (SERS) is a powerful analytical strategy that can provide fingerprint information of analytes, and it has also been considered to be an ultra-sensitive label-free detection method in various fields.[8–10] More importantly, the SERS technique exhibits narrow emission bands, demonstrating advantages in complex specimens. In SERS, the light excitation of surface plasmon resonances can significantly enhance the localized electromagnetic field at nanoscale "hot spots".[11,12] Typically, owing to the random distribution of hot spots on the SERS substrate, the SERS signals indicate poor reproducibility. Therefore, the challenge is to reproducibly fabricate a nanostructure with uniform gaps. Jwa-Min Nam *et al.* reported that DNA on gold nanoparticles facilitated the formation of well-defined gold nanobridged nanogap particles (Au-NNPs), which generated a highly stable and reproducible SERS signal.[13] Bongsoo Kim *et al.* fabricated an SERS platform composed of single metallic nanowire (NW) on a metallic film with optical location and high reproducibil-

[a]Department of Chemical and Materials Engineering, Hefei University, HefeiAnhui, 236061, China. E-mail: wuyp@hfuu.edu.cn
[b]Institute of Intelligent Machines, Chinese Academy of Sciences, Hefei, 230031, China. E-mail: lipan2011@iim.ac.cn
†Electronic supplementary information (ESI) available: The SERS features of Sunset yellow. See DOI: 10.1039/c8an00540k

ity.[14] Jürgen Popp *et al.* used highly uniform Au "film over nanosphere" (FON) substrates together to quantitatively determine the concentration of azorubine in drinks.[15] In comparison with the above-mentioned strategies, the solution-induced self-assembly method is convenient and cost-effective. Halas *et al.* have studied cetyltrimethylammonium bromide (CTAB)-functionalized Au NPs, which form hexagonally close-packed monolayer NP arrays with uniform interparticle distance (8 nm), and these NP arrays demonstrate highly reproducible SERS signals.[16]

Herein, CTAB-modified Au NPs have been assembled into 2D films during solvent evaporation. These large-scale self-assembled Au NPs with regular and close-packed features can be used as SERS substrates, and they show excellent uniformity and large Raman enhancement factor. Using these active substrates, the sensitive detection of different food additives has been achieved. Moreover, mixtures of food additives have been measured, and the results show high sensitivity of this method. Additionally, we analyze real samples possibly containing the illegal additives diethylhexyl phthalate (DEHP) and tartrazine. In short, these assembled active SERS substrates demonstrate high sensitivity and provide credible signals, indicating promising applications in SERS analytical fields.

Experimental section

Materials

$HAuCl_4 \cdot 4H_2O$, trisodium citrate, cetyltrimethylammonium bromide (CTAB), ascorbic acid (AA), ethanol, 4,4′-dipyridine, Rhodamine 6G (R6G), ciprofloxacin, tartrazine, azodicarbonamide and diethylhexyl phthalate (DEHP) were purchased from Sigma-Aldrich. All reagents were of analytical grade and used without further purification.

Characterizations

Ultraviolet–visible (UV-vis) absorption spectra were obtained using a Shimadzu UV-2550 spectrophotometer (Japan), and the background spectrum was deducted. Scanning electron microscopy images were obtained using a field-emission scanning electron microscope (Quanta 200FEG). Raman spectra were recorded using a LabRAM HR800 confocal microscope Raman system (Horiba JobinYvon) with a 633 nm He–Ne laser source. The laser was focused with a LWD 50/0.5 NA objective lens, and the laser spots had a diameter of about 1.5 μm with laser power of approximately 0.5 mW.

Synthesis of Au NPs

The synthesis of Au NPs is described by a seed-growth method. First, 1 mL of $HAuCl_4 \cdot 4H_2O$ (1%) aqueous solution was diluted with 90 mL of water and then boiled with vigorous stirring. Then, 4 mL of aqueous citrate (1%) solution was used as a reductant, and it was quickly added. This solution was used as Au seeds (∼15 nm) to prepare larger Au NPs. Second, the growth solution 10 mL $HAuCl_4 \cdot 4H_2O$ (9.6×10^{-4} M), reductant solution 10 mL citrate (9.7×10^{-4} M), and AA (2.84×10^{-3} M)

were added to the above-mentioned solution (15 mL) at the rate of 0.23 mL min^{-1}, which resulted in the formation of Au NPs 50 nm in diameter. Then, the growth solution 10 mL $HAuCl_4 \cdot 4H_2O$ (9.6×10^{-4} M), reductant solution 10 mL citrate (9.7×10^{-4} M), and AA (2.84×10^{-3} M) were added to the obtained Au NPs having a size of 50 nm (4 mL) at the rate 0.23 mL min^{-1}, which resulted in the formation of Au NPs 80 nm in diameter.
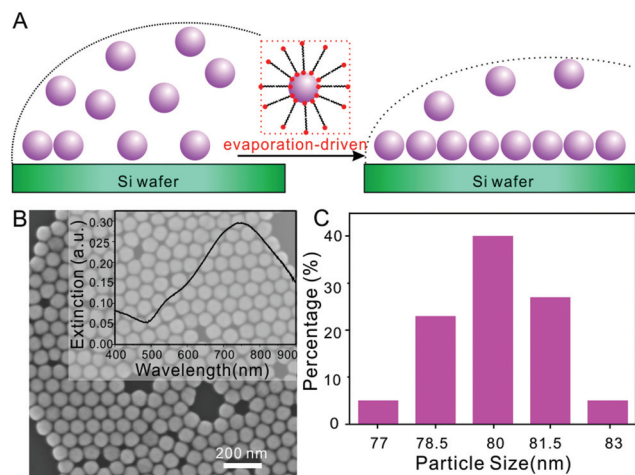
Assembly of Au NPs

Citrated stabilized Au NPs (15 mL) were concentrated by centrifuging at 4500 rpm for 10 min. After that, the supernatant was removed, and the residue was re-dispersed in H_2O (total volume 15 mL). The solution was stirred slowly for 6 h after CTAB (25 mM) was added. Then, 1 mL of CTAB-functionalized Au NPs was centrifuged at 4500 rpm for 10 min and then, excess CTAB was removed and the residue was re-dispersed in 0.2 mL H_2O. Finally, a 5 μL droplet of CTAB-functionalized Au colloid solution dried on a silicon wafer under ambient conditions resulted in the formation of close-packed monolayer Au NP arrays.

SERS measurement

Aqueous solutions of 4,4′-dipyridine, Rhodamine 6G, ciprofloxacin, tartrazine, azodicarbonamide and DEHP having concentrations of 10^{-3}, 10^{-4}, 10^{-5}, 10^{-6}, 10^{-7}, and 10^{-8} M, respectively, were prepared. During the SERS measurements, 10 μL aliquots of the above-mentioned analytes were added onto the Au NP array and dried naturally at room temperature. Ethanol solutions of DEHP at 10^{-3}, 10^{-4}, 10^{-5}, 10^{-6}, 10^{-7} and 10^{-8} M were prepared and then, 10 μL aliquots of DEHP solutions were added onto the Au NP arrays for measurements. Commercial liquors and commercial sweet drinks were directly added onto the assembled Au NP arrays for further measurements and analysis without pre-treatment. During the SERS measurements, 10 μL of commercial liquor or commercial sweet drink was added onto the Au NP array and dried naturally at room temperature.
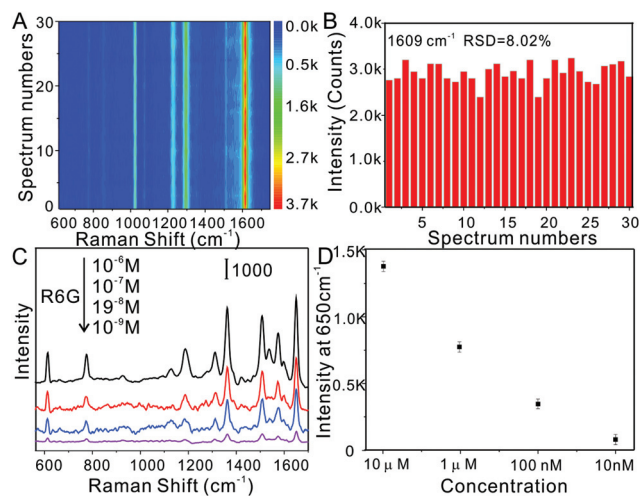
Results and discussion

In recent decades, many efforts have been made to develop a novel strategy for assembling colloids to fabricate SERS-active substrates with strong plasmonic response and high reproducibility.[17–20] Among these methods, evaporation-driven methods have been widely explored because they can achieve the synthesis of high-quality planar colloidal films. Thus, in this report, an evaporation-driven self-assembly method to form Au NP films is given, and it is exhibited in Fig. 1A. The adopted self-assembly method for creating nanoparticle films is quite simple and robust. Herein, Au NPs are used as building blocks for SERS substrates because of their plasmonic activities and stable properties. The self-assembly of monolayer Au NP arrays by solvent evaporation mainly consists of two-stages: nucleus formation and crystal growth, which contain attractive capillary forces and convective particle flux to

Fig. 1   (A) Schematic of solvent evaporation-driven self-assembly of Au NPs. (B) SEM image of self-assembled Au NP film; inset shows the extinction spectrum of Au NP assemblies. (C) Size distribution of Au NPs.

Fig. 2   (A) 2D-SERS mapping of 4,4′-dipyridine (1 μM) and (B) the variation of SERS intensity of the Raman modes at 1609 cm^{-1} (the relative standard deviation (RSD) is 8.02%). (C) SERS spectra of Rhodamine 6G with different concentrations and (D) R6G intensity at 1650 cm^{-1} as a function of R6G concentration. The error bar is from three independent measurements.

govern the ordered array. Furthermore, the ordered monolayer of a nanoparticle is controlled by the water evaporation rate. Herein, CTAB as a kind of surfactant reduces the evaporation rate compared with pure water under the same conditions; meanwhile, its steric feature enables hard-sphere-like interactions between adjacent nanoparticles, which facilitates the formation of highly uniform monolayer arrays. As shown in Fig. 1B, the field-emission scanning electron microscopy (FE-SEM) image indicates a close-packed Au NP film. During the self-assembly process, the attractive capillary force and convective flow are the governing factors, and neither electrostatic repulsion nor van der Waals attraction plays a significant role in the formation of a two-dimensional (2D) film.[21] The inset is a UV-vis spectrum of Au NPs with plasmon absorption in the range of 700–800 nm. A previous report indicates that Raman intensities increase with the increasing size of Au NPs, and the best enhancement for Au NPs is in the range from 60 to 90 nm with 632.8 nm excitation.[22] Thus, we use Au NPs with a diameter of 80 nm as the active colloids (shown in Fig. 1C).

Reproducibility is a critical issue in SERS, which always restricts the applications of the SERS technique in real samples. For this purpose, experiments evaluating the reproducibility of 2D Au NPs have been carried out. We find that the Au NP film exhibits excellent uniformity for SERS measurements. Fig. 2A shows a Raman line-scan with 30 spectra over a 10 μm scanning distance and intensities of 4,4′-dipyridine Raman peaks. Moreover, to obtain statistical data, the relative standard deviation (RSD) of the main vibration at 1609 cm^{-1} is 8.02%, which is consistently less than 20%, indicating that the self-assembled substrates show excellent reproducibility. It is worth emphasizing that the measurement region mentioned above is randomly selected, and consistent line or spatial uniformity can be found in the entire assembled SERS substrate. Furthermore, to confirm that this enhancement effect of the assembled substrate is generally applicable and highly sensitive, SERS spectra of Rhodamine 6G (R6G) solutions, as

Raman probes, having different concentrations ranging from 10 μM to 10 nM are shown in Fig. 2. Even at the nM level, the characteristic SERS spectra of R6G can be obviously distinguished. Also, the plot of the normalized R6G intensity at 1650 cm^{-1} *versus* different concentrations is obtained with good line correlation. Furthermore, to demonstrate the stability of SERS substrates, the SERS performances of the corresponding control experiment for different batches of substrate after one month of storage time have been shown in Fig. S2.† Based on the above-mentioned analysis, this self-assembled substrate indicates excellent sensitivity and reproducibility; hence, it can act as an active SERS platform for the highly sensitive detection of food additives.
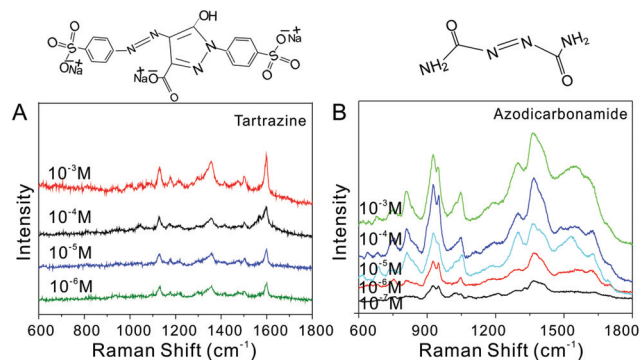
Furthermore, antibiotics can be pathogenic and dangerous to both humans and animals.[23] This issue has motivated analytical chemists toward the development of sensitive and reliable sensors to monitor traces of antibiotics and metabolites. Considering the advantages of the SERS technique, which include rapid response and high sensitivity, Brolo et al.[24] fabricated periodic metallic nanostructures using laser interference lithography (LIL) for use as SERS substrates in the sensitive detection of ciprofloxacin at the ppm level. Also, Zhao et al.[25] developed a method for fast extraction and ultrasensitive detection of ciprofloxacin based on magnetic-imprinted SERS strategy at the 0.1 ppm level. In this report, using the self-assembled Au NP film as SERS platform, a highly sensitive detection of ciprofloxacin is achieved. Fig. 3A shows the SERS spectra of ciprofloxacin with different concentrations ranging from 10^{-3} M to 10^{-8} M. Even at the 10 nM level, the SERS features of ciprofloxacin can be distinguished. The band at 747 cm^{-1} is assigned to methylene rocking, the band at 1391 cm^{-1} is assigned to C–O stretching, and the band at 1627 cm^{-1} is assigned to carboxyl stretching. Phthalic
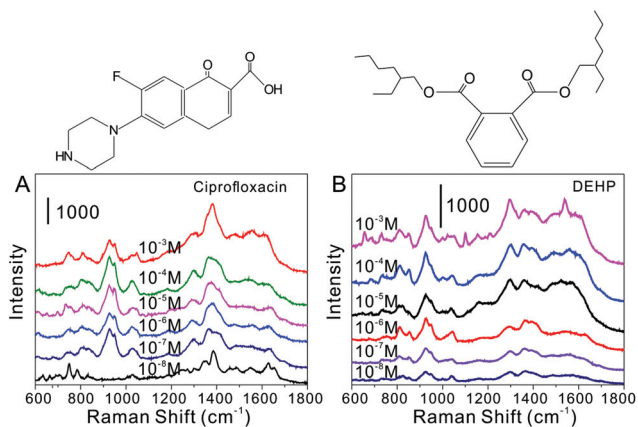
Fig. 3 (A) SERS features of ciprofloxacin and (B) DEHP with concentration ranging from 10^{-3} M to 10^{-8} M as well as their molecular structures.

Fig. 4 (A) SERS features of tartrazine with concentration ranging from 10^{-3} M to 10^{-6} M and (B) SERS features of azodicarbonamide with concentration ranging from 10^{-3} M to 10^{-7} M as well as their molecular structures.

acid esters (PAEs) are most widely used in industrial production as additives. During their production and utilization, PAEs can diffuse everywhere such as in water, food and rainwater, which also causes human endocrine system disorders.[26,27] As a result, the sensitive detection of diethylhexyl phthalate (DEHP) has been carried out. As shown in Fig. 3B, we use a uniform Au NP film to analyze trace DEHP diluted in ethanol. Besides bands for various vibrations of C–C–C ring, C–H and C–C, the bands associated with vibrations of the orthophenyl group at 659, 1040, and 1574 cm^{-1} can be clearly identified. These results demonstrate that this self-assembled Au NPs array has great potential as a highly sensitive SERS substrate for the detection of antibiotics and PAEs.

Besides the addition of various antibiotic additives, to increase the visual attractiveness and to restore the original appearance of food products and drinks, different food colorants or additives are added.[28,29] However, some of the additive colorants demonstrate potential risks to human health, especially in the case of excessive consumption.[30,31] For example, tartrazine as food colorant has been widely used as an artificial food and drink additive. Possible effects on human health are reported due to the unavoidable presence of carcinogenic β-naphthylamine. Typically, tartrazine is a permitted food colorant with maximum use level of 50–500 μg g^{-1}.[32] The chemical formula of tartrazine is $C_{16}H_9N_4O_9S_2Na_3$, and it usually exists in the form of non-crystalline water. Using the CTAB-functionalized Au NP films, the SERS features of tartrazine are obtained. Fig. 4A exhibits SERS spectra of tartrazine with concentration ranging from 10^{-3} M to 10^{-6} M. Due to the high affinity of tartrazine towards the uniform active SERS-enhanced substrates, high sensitivity is realized, which can help the detection of food additives. On the other hand, this assembled Au NPs also indicate high sensitivity for the food colorant Sunset yellow at the ppm level (shown in Fig. S1†). In addition to food colorants, because of the bleaching and oxidability of azodicarbonamide, it is always used as a flour bleaching agent in flour products such as

steamed bread.[33] In China, as a food additive, the maximum amount of azodicarbonamide allowed in flour is 45 μg g^{-1}. Nonetheless, it has been deemed to be as toxic as melamine and Sudan Red in Europe and Japan. It is reported that azodicarbonamide is classified as a toxic and illegal food additive in several countries. Herein, the SERS spectra of azodicarbonamide at different concentrations can be obtained. As shown in Fig. 4B, the Raman peak located at 816 cm^{-1} is assigned to δ(N–H), and a band around 957 cm^{-1} is from ν(C–N═N) + δ(C–N). δ(H–N–H) + ν(C═O) + ν(C–N) contribute to a peak at 1058 cm^{-1}, and a band at 1350 cm^{-1} is assigned to ν(C–N) + δ(N–C═O). Also, the 0.1 ppm target molecule can be obviously distinguished, providing potential for the sensitive detection of the additive azodicarbonamide in real specimens.

To prove the potential of our approach for detecting different additives in complex matrices, we tested several commercial liquors and sweet drinks. In complex matrices, the SERS technique suffers from serious interferences from the matrix compositions.[34,35] Nonetheless, it possesses the distinct advantages of narrow emission bands, avoiding spectral multiplexing and the weaker Raman cross-section of water, which provides more opportunities for SERS in complex specimens. It is worth noting that the amount of PAEs in the liquor of "Jiu Gui" was excessive in 2012, and it spread in all other liquor products. Moreover, PAEs in liquor come from the migration of various plastic materials during the production process, mainly from the plastic liquor tubes. Therefore, we tested two commercial sorghum and erguotou liquors. As shown in Fig. 5A, DEHP assigned to PAEs exhibited SERS features at 802, 855, 927, 1292 and 1585 cm^{-1}. Surprisingly, the characteristic bands located at 802, 855, and 927 cm^{-1} could be distinguished from those of commercial sorghum liquor and erguotou liquor, which revealed that these liquors possibly contained PAEs. On the other hand, commercial sweet drinks were selected to detect the addition of food colorants. It is known that food colorants are added to sweet drinks to increase their visual attractiveness and to restore their original appearance. Herein, we obtained SERS spectra of the com-
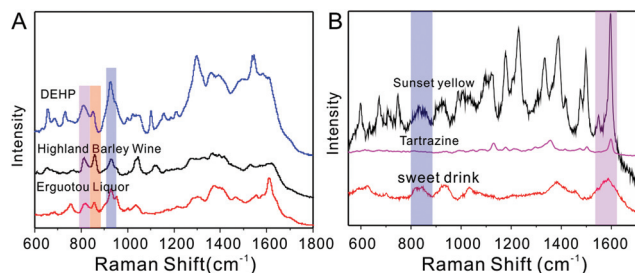
Fig. 5 (A) SERS features of DEHP collected from different samples: 10^{-8} M pure DEHP dissolved in ethanol (blue line), two commercial liquors of highland barley wine (black line) and erguotou liquor (red line). (B) SERS features of Sunset yellow (10^{-6} M, black line), tartrazine (10^{-6} M, purple line) and the commercial sweet drink (red line).

monly used colorants Sunset yellow and tartrazine, and the SERS features were mainly located in the range of 1000–1600 cm^{-1}. The SERS spectra of sweet drinks did not have the corresponding bands, indicating low or no addition of colorants Sunset yellow and tartrazine.

Conclusions

With the aim of a rapid and label-free detection of food additives in different commercial products by the SERS method, we fabricated a large-scale uniform Au NP film using the solvent-driven self-assembly strategy. This active substrate exhibited sensitivity and reliability. Moreover, the assembled Au NP films could be applied for the sensitive analysis of antibiotics, PAEs and colorants in different liquors and sweet drinks without any pre-treatment of the samples or functionalization of Au NPs. Consequently, the use of this assembled active SERS substrate may be suggested as an alternative method for realizing rapid, sensitive and credible detection of food additives in different products (using a portable Raman spectrometer) for food safety.

Conflicts of interest

There are no conflicts to declare.

Acknowledgements

References

1 L. Y. Zeng, Y. W. Pan, S. J. Wang, X. Wang, X. M. Zhao, W. Z. Ren, G. M. Lu and A. G. Wu, *ACS Appl. Mater. Interfaces*, 2015, **7**, 16781–16791.

2 N. Stone, K. Faulds, D. Graham and P. Matousek, *Anal. Chem.*, 2010, **82**, 3969–3973.

3 M. L. Xu, Y. Gao, X. X. Han and B. Zhao, *J. Agric. Food Chem.*, 2017, **65**, 6719–6726.

4 S. Kolusheva, O. Molt, M. Herm, T. Schrader and R. Jelinek, *J. Am. Chem. Soc.*, 2005, **127**, 10000–10001.

5 H. Y. Liang, Z. P. Li, Z. X. Wang, W. Z. Wang, F. Rosei, D. L. Ma and H. X. Xu, *Small*, 2012, **8**, 3400–3405.

6 J. H. Duan and Z. H. Yuan, *J. Agric. Food Chem.*, 2001, **49**, 1087–1089.

7 S. Samanta, C. Kar and G. Das, *Anal. Chem.*, 2015, **87**, 9002–9008.

8 W. K. Kowalchyk, K. L. Davis and M. D. Morris, *Spectrochim. Acta, Part A*, 1995, **51**, 145–151.

9 H. B. Zhou, D. T. Yang, N. P. Ivleva, N. E. Mircescu, R. Niessner and C. Haisch, *Anal. Chem.*, 2014, **86**, 1525–1533.

10 X. H. Li, J. M. Zhu and B. Q. Wei, *Chem. Soc. Rev.*, 2016, **45**, 4032–4032.

11 Y. J. Liu, S. Pedireddy, Y. H. Lee, R. S. Hegde, W. W. Tjiu, Y. Cui and X. Y. Ling, *Small*, 2014, **10**, 4940–4950.

12 K. A. Willets, S. M. Stranahan and M. L. Weber, *J. Phys. Chem. Lett.*, 2012, **3**, 1286–1294.

13 D. K. Lim, Ki. S. Jeon, J. H. Hwang, H. Kim, S. Kwon, Y. D. Suh and J. M. Nam, *Nat. Nanotechnol.*, 2011, **6**, 452–460.

14 I. Yoon, T. Kang, W. Choi, J. Kim, Y. Yoo, S. W. Joo, Q. H. Park, H. Ihee and B. Kim, *J. Am. Chem. Soc.*, 2009, **131**, 758–762.

15 V. Peksa, M. Jahn, L. Štolcová, V. Schulz, J. Proska, M. Procházka, K. Weber, D. Cialla-May and J. Popp, *Anal. Chem.*, 2015, **87**, 2840–2844.

16 H. Wang, C. S. Levin and N. J. Halas, *J. Am. Chem. Soc.*, 2005, **127**, 14992–14993.

17 R. H. Que, M. W. Shao, S. J. Zhuo, C. Y. Wen, S. D. Wang and S. T. Lee, *Adv. Funct. Mater.*, 2011, **21**, 3337–3343.

18 A. Q. Chen, A. E. DePrince, A. Demortiere, A. Joshi-Imre, E. V. Shevchenko, S. K. Gray, U. Welp and V. K. Vlasko-Vlasov, *Small*, 2011, **7**, 2365–2371.

19 K. Sugawa, T. Akiyama, Y. Tanoue, T. Harumoto, S. Yanagida, A. Yasumori, S. Tomita and J. Otsuki, *Phys. Chem. Chem. Phys.*, 2015, **17**, 21182–21189.

20 Y. Tanoue, K. Sugawa, T. Yamamuro and T. Akiyama, *Phys. Chem. Chem. Phys.*, 2013, **15**, 15802–15805.

21 A. El Bakkali, T. Lamhasni, M. Haddad, S. A. Lyazidi, S. Sanchez-Cortes and E. D. Nevado, *J. Raman Spectrosc.*, 2013, **44**, 114–120.

22 G. K. Liu, P. C. Zheng, G. L. Shen, J. H. Jiang, R. Q. Yu, Y. Cui and B. Ren, *J. Phys. Chem. C*, 2010, **112**, 6499–6508.

23 M. H. Li, H. Wu, Y. P. Wu, Y. Ying, Y. Wen, X. Y. Guo and H. F. Yang, *J. Raman Spectrosc.*, 2017, **48**, 525–529.

24 K. Y. Hong, C. D. L. de Albuquerque, R. J. Poppi and A. G. Brolo, *Anal. Chim. Acta*, 2017, **982**, 148–155.

25 Z. A. Guo, L. Chen, H. M. Lv, Z. Yu and B. Zhao, *Anal. Methods*, 2014, **6**, 1627–1632.

26 Q. Cao and R. C. Che, *ACS Appl. Mater. Interfaces*, 2014, **6**, 7020–7027.

27 Z. W. Zuo, K. Zhu, L. X. Ning, G. L. Cui, J. Qu, Y. Cheng, J. Z. Wang, Y. Shi, D. S. Xu and Y. Xin, *Appl. Surf. Sci.*, 2015, **325**, 45–51.

28 F. Pozzi, S. Zaleski, F. Casadio and R. P. Van Duyne, *J. Phys. Chem. C*, 2016, **120**, 21017–21026.

29 Z. Sun, J. Du, L. Yan, S. Chen, Z. Yang and C. Jing, *ACS Appl. Mater. Interfaces*, 2016, **8**, 3056–3062.

30 J. Meng, S. Qin, L. Zhang and L. B. Yang, *Appl. Surf. Sci.*, 2016, **366**, 181–186.

31 Y. Xie, T. Chen, Y. Cheng, H. Wang, H. Qian and W. Yao, *Spectrochim. Acta, Part A*, 2014, **132**, 355–360.

32 V. Peksa, M. Jahn, L. Stolcova, V. Schulz, J. Proska, M. Prochazka, K. Weber, D. Cialla-May and J. Popp, *Anal. Chem.*, 2015, **87**, 2840–2844.

33 M. Li, X. Guo, H. Wang, Y. Wen and H. Yang, *Sens. Actuators, B*, 2015, **216**, 535–541.

34 Y. Ma, H. Liu, M. Mao, J. Meng, L. Yang and J. Liu, *Anal. Chem.*, 2016, **88**, 8145–8151.

35 F. Sun, H. C. Hung, A. Sinclair, P. Zhang, T. Bai, D. D. Galvan, P. Jain, B. W. Li, S. Y. Jiang and Q. M. Yu, *Nat. Commun.*, 2016, **7**, 13437.